



Synthesis, Characterization and Antimicrobial Activity Study of the Ternary (Poly Anthranilic acid- Graphene Oxide- Zinc Oxide) Nanocomposite

Abdulwahhab H. Majeed 

Department of Chemistry, College of Science, University of Diyala, Diyala, Iraq

abdulwahhab@uodiyala.edu.iq

This article is open-access under the CC BY 4.0 license (<http://creativecommons.org/licenses/by/4.0>)

Received: 11 December 2023

Accepted: 22 January 2024

Published: January 2025

DOI: <https://dx.doi.org/10.24237/ASJ.03.01.839B>

Abstract

In this study, a (Poly anthranilic acid (PANA) - Graphene Oxide (GO) nanosheets, Zinc Oxide (ZnO) nanorods) ternary nanocomposite was synthesized. The prepared compounds (PANA, GO, ZnO and the (PANA-GO-ZnO) nanocomposite were characterized through Fourier transform infrared (FTIR), X-Ray diffraction (XRD), scanning electron microscope (SEM), and thermal analysis. The analyses revealed that GO consisted of nanostructures in sheet form, ZnO consisted of rod-shaped structures with dimensions varying between 39 and 63 nm, and the polymer appeared in regular, sphere-like shapes with different diameters. Thermal analysis of the polymer showed that the polymer (PANA) partially decomposes in the temperature range (145.3-315.6 °C), and completely decomposes at (315.6, 541.9 °C). The ternary nanocomposite was employed to assess their efficacy against four distinct bacterial strains (Staphylococcus aureus, Staphylococcus epidermidis, Escherichia coli, and Klebsiella sp.) and one fungal strain (Candida albicans). It was also found that this compound has a high effectiveness in inhibiting the tested microorganisms.

Keywords: Graphene Oxide, Poly anthranilic acid, ZnO, Ternary Nanocomposite, Antimicrobial activity.



Introduction

Every year, a large number of people throughout the world succumb to severe sickness, blood poisoning, and infections brought on by bacteria and other microbes. The advent of multidrug-resistant bacteria has been prompted by the extensive use of antibiotics, which were formerly a standard tactic in the fight against bacterial diseases. In light of these ever-changing threats, it is critical to develop more effective and technologically advanced antibiotics. An alternate strategy for combating antibiotic resistance is preventing its emergence in the first place by limiting the ability of bacteria to multiply on various substrates. One way to accomplish this is to stop them from attaching or to slow down their development. Here, one potentially fruitful tactic is the search for and creation of novel antibacterial materials [1].

There is a growing interest in polymers and polymer-based materials due to their critical roles in many applications, particularly in the biomedical sector. Medicinal materials must possess antibacterial capabilities, which are among the most important criteria. It is critical to stop the growth of bacteria on surgical masks, urinary and intravenous catheters, prosthetics, and other medical equipment in order to reduce the incidence of infections associated with these items [2]. One of the most adaptable synthetic polymers is polyaniline (PANI); it is a conjugated polymer. The exceptional environmental stability, ease of manufacturing, and straightforward doping/dedoping chemistry are its commonly reported features. Thereby, it was a good candidate for different applications, such as the artificial muscle technology, regulated medication delivery, and improved neuron regeneration. However, it is also important to consider the conductive cotton textiles treated with PANI and their antibacterial and antifungal qualities [3]. The application of PANI as an electron donor and an electron acceptor is unique; this property might account for its antibacterial actions. This could be attributed to the electrostatic interaction between the bacteria and the polymer molecules. The two chemicals' polarization charges are incompatible with one another. Hence, as the bacteria undergo this process, their cell walls break down, releasing intracellular fluid and eventually killing the bacterium [4].

One form of graphene that has piqued the interest of scientists is graphene oxide (GO), which has a distinctive hexagonal atomic structure. The unique characteristics of graphene nanosheets,



including their high aspect ratio and sharp edges, are the basis for the antibacterial and antimicrobial capabilities of graphene oxide (GO) and reduced graphene oxide (rGO). These features make it easier to rupture cell membranes and liberate intracellular contents [5]. Latest studies highlight the appreciable antimicrobial effects of metal and metal oxide composites, such as ZnO, TiO₂, Ag and Ag₂O, Si, Au, Cu, MgO, SiO₂, CuO, and CaO, against waterborne microbes [6]. Different combinations of graphene oxide and metal oxides, exemplified by TiO₂/GO, have demonstrated the ability to impede the growth of *Escherichia coli* [7] and *Caenorhabditis elegans* nematodes [8], GR/ZnO/ [9], and rGO/Ag–ZnO [10] inhibiting *E. coli*. Notably, ZnO-graphene oxide emerges as a particularly effective antimicrobial agent. ZnO acts externally on cells, releasing reactive cell content, and helping Drug Administration [11]. Mohsen, Ragia M., et al. conducted the synthesis of nanocomposites consisting of Polyaniline and zinc oxide (PANI/ZnO NCs) through the chemical oxidative polymerization of aniline. This process occurred in a dispersion containing varying weight percentages of ZnO nanoparticles (NPs) – specifically, 1.5%, 3%, 5%, and 8% in relation to aniline. The ZnO NPs were produced using the combustion method. The antibacterial efficacy of these nanocomposites against *Escherichia coli* and *Staphylococcus aureus* was assessed. A moderate level of antibacterial activity against *E. coli* was observed across all NCs. Notably, the formulation containing 8% ZnO exhibited elevated antibacterial activity against *Staphylococcus aureus* [12].

Tariq, Muhammad, et al., utilized a green synthesis approach to create a ZnO@GO nanocomposite by decorating zinc oxide onto graphene oxide. Transmission Electron Microscopy (TEM) analysis confirmed the successful synthesis of small-sized trigonal ZnO on the surface of GO nanosheets. The resulting ZnO@GO composite exhibited excellent antibacterial activity against a multidrug-resistant gram-negative pathogen, *E. coli* (BL21 DE3), eliminating around 95% of the bacteria within 5 hours. This effectiveness was attributed to the electrostatic interaction between the cell membrane of *E. coli* (BL21 DE3) and the ZnO@GO complex [13]. Zhong, Linlin, and Kyusik Yun employed a cost-effective and high-yield solution precipitation method to produce nanosized ZnO particles with a 15 nm diameter. Dimethylformamide, an organic solvent, was utilized to functionalize the particle synthesis, and the particles were covalently linked to graphene oxide surfaces. The resulting ZnO/graphene



oxide composites exhibited notable antibacterial activity, with microdilution method-determined minimum inhibitory concentrations of 6.25 $\mu\text{g/mL}$ for *Escherichia coli* and *Salmonella typhimurium*, 12.5 $\mu\text{g/mL}$ for *Bacillus subtilis*, and 25 $\mu\text{g/mL}$ for *Enterococcus faecalis* [14].

It is expected that when graphene oxide - zinc oxide is combined with polyaniline or one of its derivatives (such as poly anthranilic acid), this will lead to a significant improvement in inhibiting the growth of these microbes due to the complex dual effect that these nanocomposites exhibit towards different microbes. Therefore, in this study, GO, ZnO and PANA were prepared. From these compounds, the (PANA-GO-ZnO) nanocomposite is prepared. These compounds are characterized using various techniques such as FTIR, XRD, SEM and thermal examinations. These prepared compounds are also used against different types of bacteria and fungi.

Experimental

Chemicals:

The study utilized solvents and chemicals obtained from different suppliers, including Riedel-de Haën, Sigma-Aldrich, or SDH. These substances were used as received without undergoing any modification or purification.

Methods:

1. Synthesis of graphene oxide (GO) nanosheets:

Graphene oxide (GO) was produced through the modified Hummer method using graphite as the precursor. In a reaction flask of 250 ml was put deeply in an ice-bath at 0 °C, a mixture of 0.50 g graphite and 1.0 g sodium nitrate NaNO_3 was constantly stirred with 23 ml H_2SO_4 for 25 min. Following this, 3.0 g KMnO_4 was gradually introduced into the mixture with fast stirring at (0-5) °C. The mixture underwent moderate stirring for 1 hr. Afterward, 50 ml H_2O was cautiously added to the mixture with vigorously stirring. To further dilute the mixture, 150 ml warm H_2O was introduced, and the remaining permanganate concentrated was reduced by dissolving manganese ions through the addition of 5 ml H_2O (30%). The resulting suspension underwent filtration, multiple washes with warm distilled water, and ultrasonic treatment to exfoliate the graphene oxide into nanosheets. The nanosheets were subsequently dried in an



oven at 90°C for 24 hours to yield the graphene oxide powder. The synthesis of graphene oxide involved the utilization of graphite as the initial material through a modified Hummer method [15]–[18].

2. Synthesis of poly anthranilic acid (PANA):

Poly anthranilic acid (PANA) (2.05 g) was synthesized via the polymerization process involving anthranilic acid and ammonium persulfate (APS) (6 g) in an aqueous solution containing acetic acid, conducted at room temperature. To begin, 2.05 g of anthranilic acid was added to 50 ml of acetic acid (1 M) with continuous stirring. The oxidizing agent APS, dissolved in 50 mL of distilled water, was subsequently introduced gradually into the monomer solution. After the completion of the addition, the mixture was allowed to stir for 24 hours at room temperature. The resultant product underwent filtration, underwent multiple washes with 1M acetic acid, and was then rinsed with deionized water to eliminate any residual acetic acid. The collected precipitate was left to air-dry at room temperature for a period of 48 hours [19], [20]

3. Synthesis of zinc oxide (ZnO) nanoparticles

Zinc acetate dihydrate (2g) was gradually introduced drop by drop into a solution having 0.8 g of NaOH in 50 ml of deionized water, while stirring and heating at a temperature range of (60-65) °C. The stirring process was sustained for 3 hours, Subsequently, the mixture was left to cool in room temperature, and the resulting precipitate was then filtered, subjected to multiple washes with deionized water, and then dried in an oven at 80 °C for a duration of 8 hours [21].

4. Synthesis of binary (GO-ZnO) Nanocomposite:

For the fabrication of the binary GO-ZnO nanocomposite, 0.2 g of GO added to a 50 mL deionized water by employing an ultrasonic water bath at ambient temperature for a duration of 1 hr. Subsequently, 0.2 g of ZnO nanorods was introduced to the GO solution, and the resulting mixture was stirred for a period of 2 hrs at 25 °C before undergoing sonication for an additional hour. To obtain the isolated binary nanocomposite (GO-ZnO), the mixture was subjected to centrifugation and then dried at 85 °C for a duration of 24 hours as shown in Figure (1).

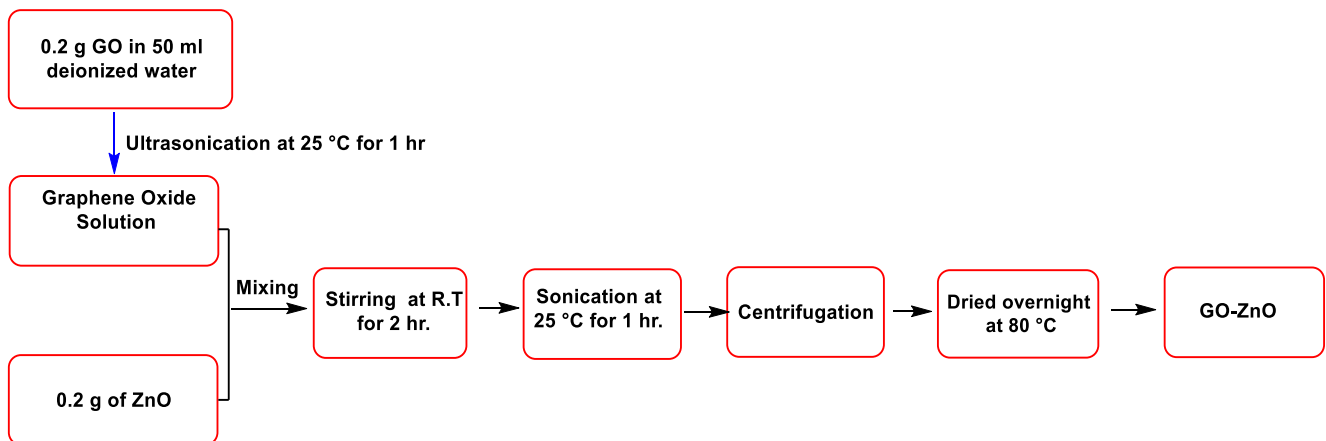


Figure 1: Schematic figure to prepare GO-ZnO nanocomposite.

5. Synthesis of ternary nanocomposite (PANA-GO-ZnO) using In-Situ polymerization:

0.5 g of the (GO-ZnO binary nanocomposite) underwent dispersion through sonication in distilled water for a duration of 1 hour. Subsequently, a solution having 1.5 g of Anthranilic acid was gradually introduced into the mixture formed in the initial step, with consistent stirring within an ice bath, and the mixture was continuously stirred for 30 minutes. Following this, an oxidizing agent solution comprising APS (4.5 g) dissolved in 80 mL of 0.1 M HCl was gradually introduced into the ultimate solution within the ice bath under continuous stir until the addition process concluded. The resulting solution was left to stir overnight. The product obtained was then subjected to filtration, washing, and ultimately drying at 85 °C for a duration of 24 hours. Figure (2) show the schematic diagram of synthesis of ternary nanocomposite (PANA-GO-ZnO).

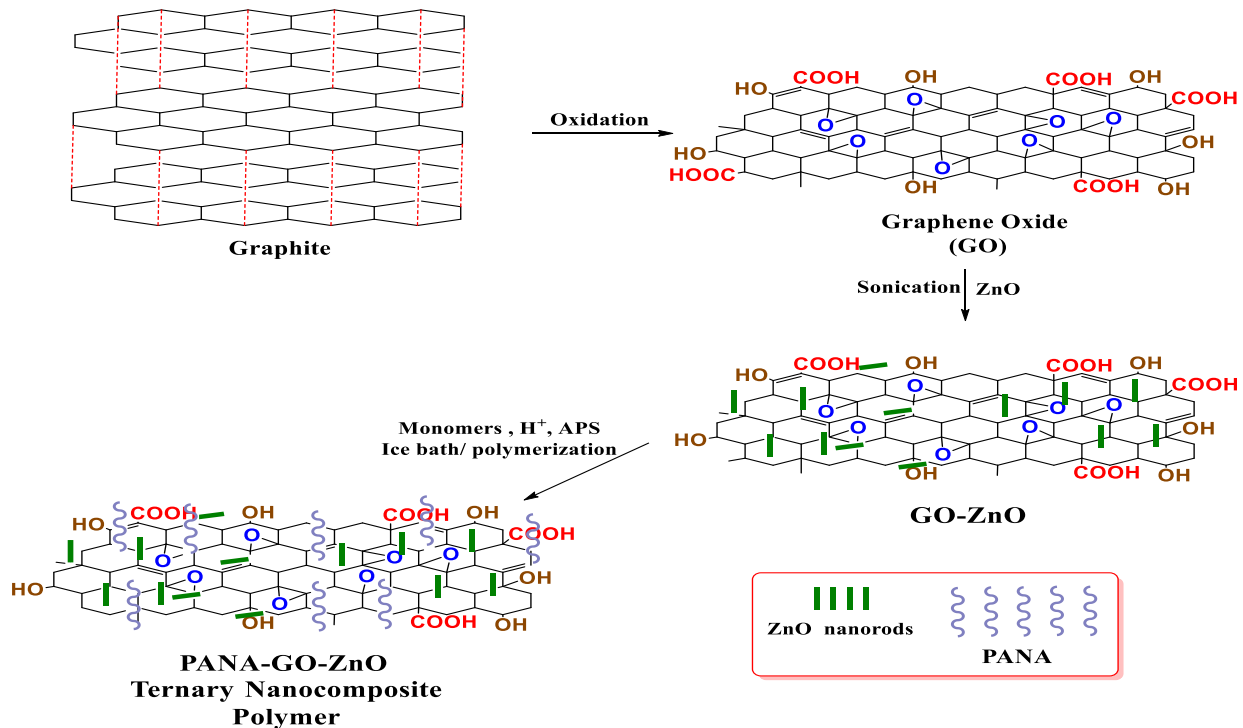


Figure 2: Synthesis of ternary nanocomposite (PANA-GO-ZnO).

Results and Discussion

Characterization:

1. FTIR:

Figure (3) shows the infrared spectrum of GO, ZnO, PANA, and PANA-GO-ZnO nanocomposite. In the FTIR spectrum of GO, distinct peaks are observed at 3426, 1726, 1623, 1223, and 1055 cm^{-1} . These peaks correspond to the stretching vibrations of ($\nu(\text{O-H})$), ($\nu(\text{C=O})$), ($\nu(\text{C=C})$) attributed to the remainder of the unoxidized graphite, epoxy groups ($\nu(\text{C-O-C})$), and alkoxy groups ($\nu(\text{C-O})$), respectively [22]. This figure illustrates the infrared spectrum of the synthesized zinc oxide nanoparticles. A distinct broad absorption band is evident at 3413 cm^{-1} , corresponding to the stretching of the O-H group of water molecules adsorbed between the zinc oxide nanoparticles. Additionally, the spectrum reveals another band at 1586 cm^{-1} attributed to the binding vibration of the O-H group of water molecules, while a band at 460 cm^{-1} is indicative of the stretching vibration of the Zn-O bond [23]. In the FTIR spectrum of PANA, distinctive bands are observed at 3365, 3195, 1685, 1580, 1507, and 1242 cm^{-1} . These bands are associated with the stretching vibrations

of O-H ($\nu(\text{O-H})$), N-H ($\nu(\text{N-H})$), C=O ($\nu(\text{C=O})$), C=C in quinoid structure ($\nu(\text{C=C quinoid})$), C=C in benzenoid structure ($\nu(\text{C=C benzenoid})$), and C-H ($\nu(\text{C-H})$), respectively [19].

Lastly, the FTIR of the ternary nanocomposite (PANA-GO-ZnO) also offered in same Figure, which has all the characteristic bands of PANA at 3220, 1690, 1560, 1499 and 1240 cm^{-1} , as well to the band at 463 cm^{-1} of Zn-O in the ZnO nanorods, respectively. It is also noted that no peaks belonging to graphene oxide appear because the polymer peaks are located in the same region as the graphene oxide peaks. Also, the polymer peaks are stronger than the GO peaks, so no clear presence of GO peaks was observed.

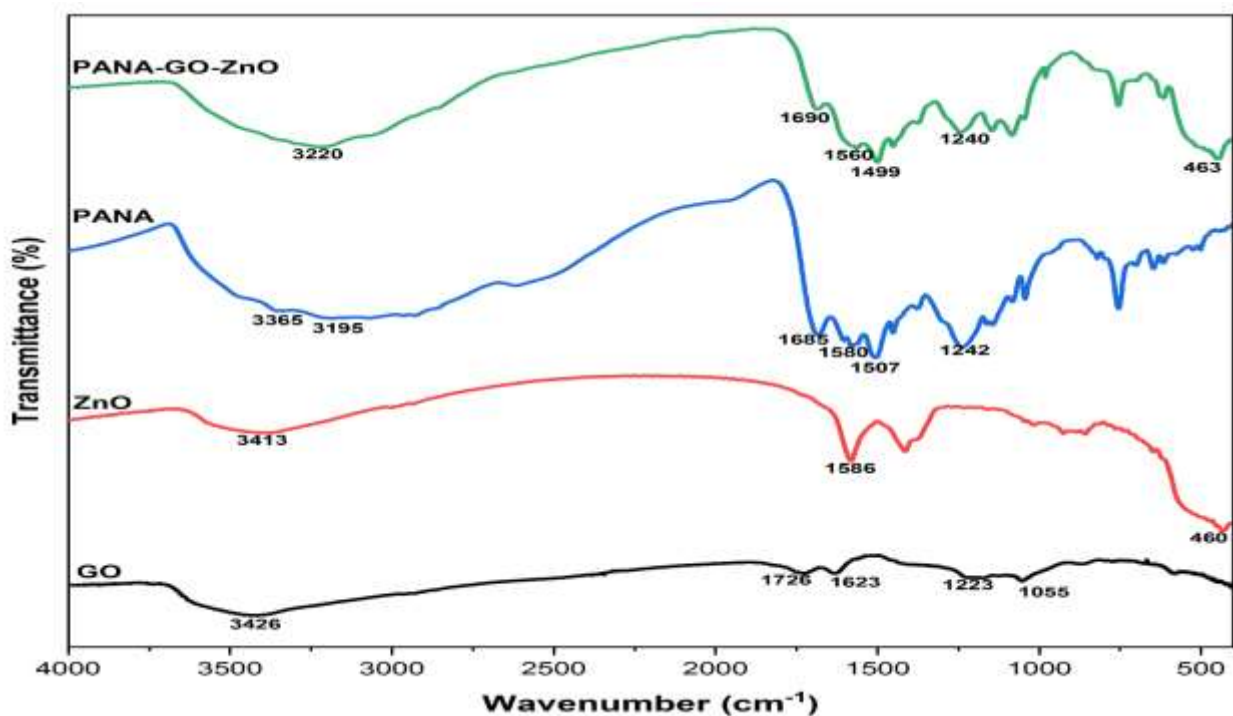


Figure 3: FTIR of GO, ZnO, PANA, and PANA-GO-ZnO nanocomposite.

2. XRD:

In Figure 4, the XRD spectra of graphite (Gt) and graphene oxide (GO), zinc oxide (ZnO) and poly anthranilic acid (PANA) are presented. The XRD analysis of graphite is crucial for discerning structural changes in the prepared graphitic materials. The XRD pattern of graphite reveals two distinct peaks at 2θ angles of 26.5° and 54.6° , corresponding to interlayer distances of 3.36 Å and 1.68 Å, respectively [24].



Conversely, the XRD examination of GO reveals a significant peak at $2\theta = 10.01^\circ$, signifying an interlayer spacing of 8.75 Å. This particular peak is linked to the existence of oxygen functional groups (including hydroxyl, carbonyl, epoxy, and carboxyl groups) formed on the sheet surfaces during the oxidation process. Furthermore, graphene oxide exhibits another peak at $2\theta = 22.4^\circ$, attributed to the partial exfoliation of the graphite [22].

In the XRD assessment of ZnO, several high-intensity bands are identified at 2θ values of 31.7° , 34.3° , 36.2° , 47.6° , 54.1° , 56.5° , 59.9° , 62.9° , 66.4° , 68.08° , 69.1° , 72.7° , and 77.1° . These findings are in concordance with existing literature ((JCPDS) Card number 36–1451)) and are consistent with previously reported research. Consequently, the synthesized zinc oxide is deemed highly pure, as there are no additional peaks observed in the examined spectrum [25]. The XRD of the pure poly anthranilic acid (PANA) shows the main peaks centered at $2\theta = 22.5^\circ$, 23.2° and 24.4° . The wide peak located at $2\theta = 24.4^\circ$ could be associated with the periodicity perpendicular to the chain(s) of the polymer. However, poly anthranilic acid shows a broad region at ($2\theta = 20\text{--}30^\circ$) demonstrating its very amorphous nature. These result give a good agreement with previously published studies [26].

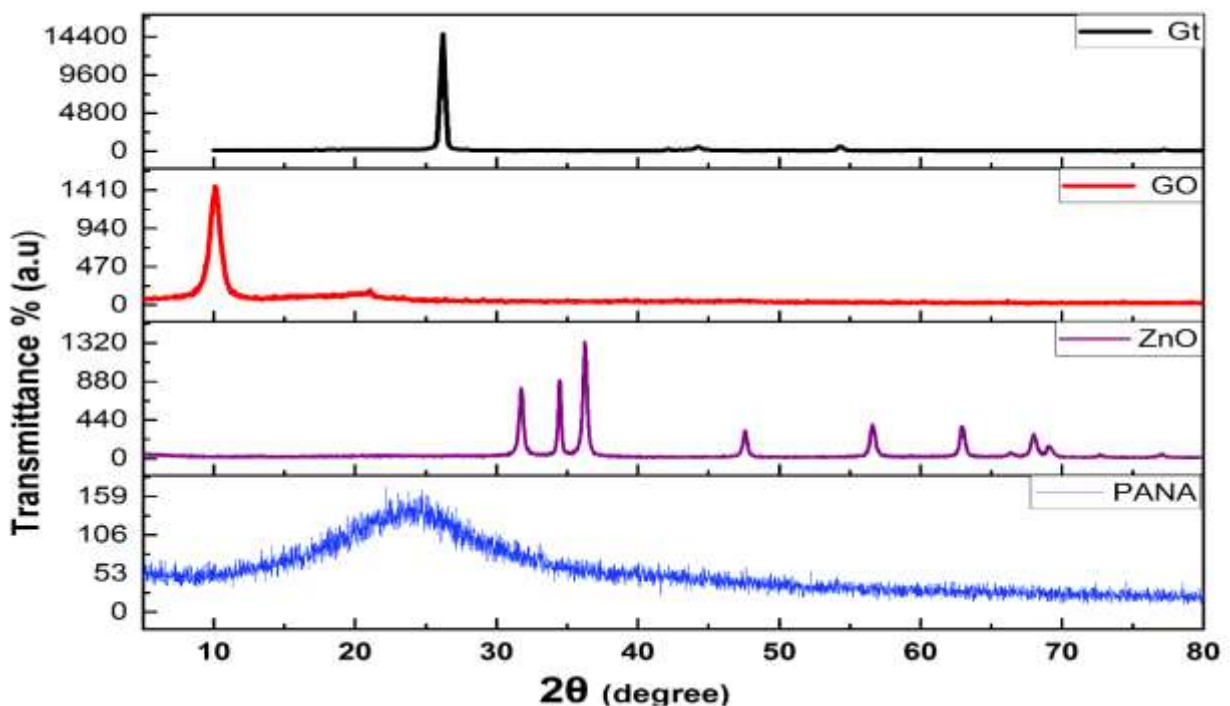


Figure 4: XRD of Gt, GO, ZnO, and PANA.



3. SEM:

The scanning electron microscope (SEM) is a sophisticated imaging tool extensively employed for examining the surface topography and dimensions of various samples at a nanoscale resolution. This technology finds a widespread application in diverse scientific fields, including materials science, nanotechnology, biology, geology, and more, aiding in comprehensive material analysis and research [27].

Figure (5) presents the SEM examination of GO nanosheets, zinc oxide (ZnO) nanorods, poly anthranilic acid (PANA), and PANA-GO-ZnO nanocomposite. From the SEM examination of GO shown in Figure (5.a), it is observed that thin and smooth sheets appear without containing any distortions contain distortions and defects on the surface of the sheet, and this indicates the success of the preparation method used. It is also noted that there are some folds on the surface of the painting, and this is the result of twisting the painting itself or the accumulation of one part of the painting on another part of it, to form this structure. As for the SEM examination of the zinc oxide nanoparticles shown in Figure (5.b), it is noted that rod-like structures appear, which are of different lengths with diameters ranging between 39-63 nanometers. The SEM examination of poly anthranilic acid displayed in Figure (5. c and d) shows a spherical microstructure with different diameters. The appearance of polymer particles in this form indicates the success of the method used, in which a long time was used for the regular growth of these particles, so the spheres seemed in a regular shape with different diameters.

On the other hand, Figure (5. e and f) shows the SEM examination of the prepared ternary nanocomposite (PANA-GO-ZnO). It is observed from the figure that sphere-like polymer structures appear on the surface of the graphene oxide sheet. It is also noted that there are a few nanorods belonging to nano-zinc oxide. The lack of a clear appearance of ZnO nanorods and graphene oxide sheets is due to the in situ polymerization process used for poly anthranilic acid, whose particles cover the surface of graphene oxide and zinc oxide structure.

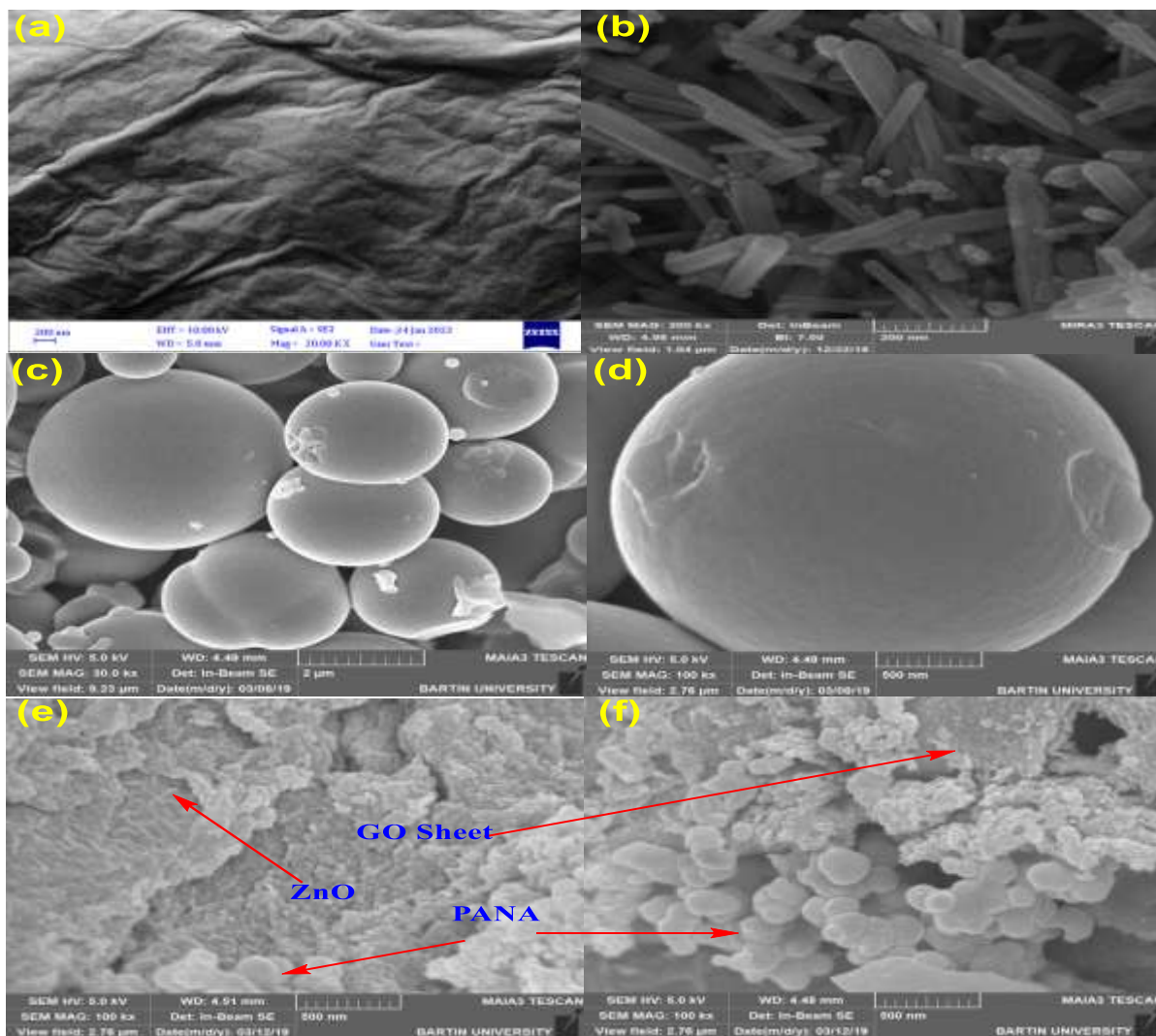


Figure 5: SEM of (a) GO, (b) ZnO, (c, d) PANA and (e, f) PANA-GO-ZnO nanocomposite.

4. Thermal analysis

The thermogravimetric (TG) plot of poly anthranilic acid exhibits four sequential weight reductions as depicted in Figure (6.a). During the initial phase, occurring between (50 - 87.6) °C, a modest weight loss of 2.7% is observed, potentially linked to the evaporation of certain water molecules situated between the polymer chains. The second stage is observed between 87.6 - 145.3 °C with a weight loss of only 4.07%. In this stage, the remaining of the water molecules are lost in addition to the oligomers and the unreacted monomer is removed. The third stage: temperature between 145.3 - 315.6 °C with a weight loss of 17.7%. The weight loss



in the third stage occurs due to partial decarboxylation of the polymer, which is attributed to the removal of carbon dioxide from the carboxyl groups in the polymer chains [28]. The final stage was found to be extensively reduced at 315.6 – 537.5 °C leaving 0.00% of the polymer with a weight of 75.53%. The decomposition at this stage is due to the complete decomposition of the poly anthranilic acid, chemical bonds and aromatic rings in the polymer. The TG% data signifies that the polymer maintains stable until reaching 315.6°C. These occurrences are particularly evident through the broad peaks in the DTG curve [26].

The thermogravimetric (TG) plot of the PANA-GO-ZnO nanocomposite in Figure (6.b) illustrates four successive weight reductions with rising temperature. In the initial phase, occurring between 50-93.3 °C, a modest weight loss of 4.7% is observed, attributed to the evaporation of water molecules potentially adsorbed on the high surface area of the nanoparticles (GO and ZnO). As for the second stage, it was observed between 93.3-277.3 °C with a weight loss of only 8.9%. In this stage, oligomers are lost, and the unreacted monomer and the rest of the water fragments that may be adsorbed on the high surface area of the nanoparticles (GO and ZnO) are removed. As for the third stage, it decreased more widely at a temperature of 277.3 - 403.2 °C, with a weight loss of 27.1%. At this stage, partial decomposition of the polymer occurs, as well as loss of some oxygen groups from graphene oxide. The fourth stage appeared at 403.2-515.5 °C, with a weight loss of 19.6%. These may be attributed to the total decomposition of the polymer and the partial decomposition of graphene oxide. As for the last stage, 515.5 - 700 °C, the undecomposed materials (39.7%) at (515.5 – 700 °C) can be attributed to ZnO and coal [22]. These events are most clearly visible by the broad peaks in the DTG pattern.

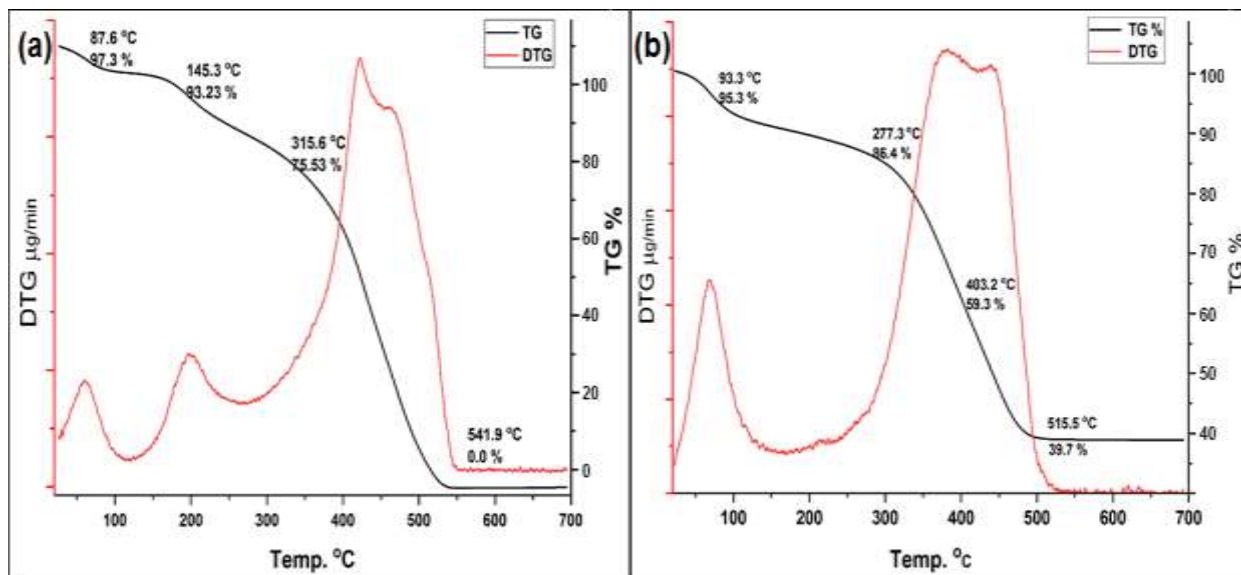


Figure 6: Thermal analysis of PANA and PANA-GO-ZnO nanocomposite.

5. Antimicrobial activity:

The anti-bacterial activity of new ternary compound (PANA-GO-ZnO) with 10 mg/ml of Dimethyl sulphoxide (DMSO) as a solvent was examined by using the agar well diffusion method on Muller Hinton agar medium with MacFarland turbidity as a standard solution. The zones of inhibition exhibited by the tested compound was measured in (mm), as shown in Table (1) which presents the findings. The screening results showed the compound (PANA-GO-ZnO) has high activity against all microorganisms (Staphylococcus aureus, Staphylococcus epidermidis, Escherichia coli, Klebsiella sp. and Candida albicans) as shown in Figure (7).

Table 1: The inhibition zones of the PANA-GO-ZnO nanocomposite.

Microorganism	Diameters of the inhibition (mm)	
Gram-positive bacteria	Staphylococcus aureus	81
	Staphylococcus epidermidis	> 90
Gram-negative bacteria	Klebsiella pneumonia	69
	Escherichia coli	71
fungal strain	Candida albicans	37

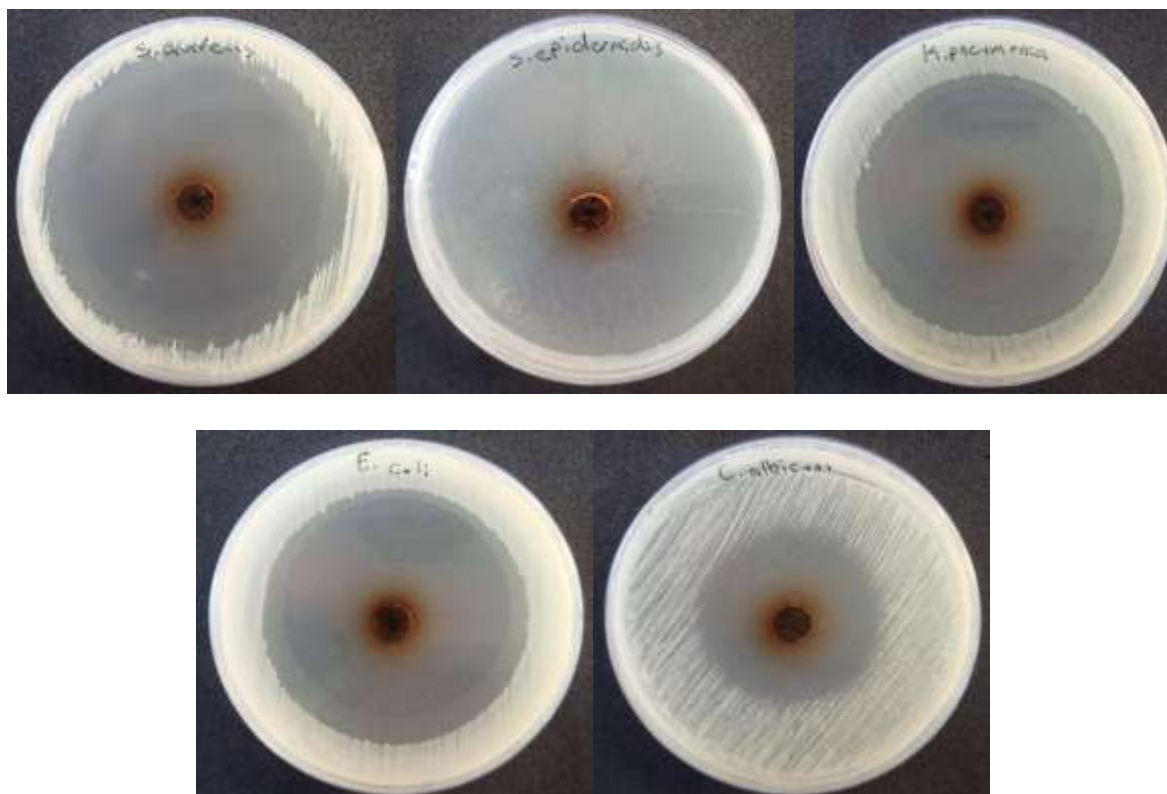


Figure 7: Effects of the PANA-GO-ZnO nanocomposite against the microorganisms.

Conclusions

The prepared compounds (GO, ZnO, PANA and PANA-GO-ZnO nanocomposite) were characterized using various spectroscopic methods such as FT-IR, XRD and SEM, as well as using thermal tests (TG) to determine the thermal stability of the polymer and the ternary composite. Through analyses, the chemical composition of the prepared materials was proven, and from SEM measurement it was found that GO was prepared in the form of nanosheets. ZnO was prepared in the form of nanorods, and poly anthranilic acid was prepared in the form of balls with different diameters. Thermogravimetric (TG) analysis was also used to study the thermal decomposition of the polymer with temperature. It was found that the polymer is stable up to approximately 300°C. In addition, the antimicrobial activity of the PANA-GO-ZnO was measured. It was found that the compound has high effectiveness in inhibiting the microorganisms (Staphylococcus aureus, Staphylococcus epidermidis, Escherichia coli, Klebsiella sp. and Candida albicans).



References

1. N. F. Kamaruzzaman, Antimicrobial polymers: the potential replacement of existing antibiotics?, *Int. J. Mol. Sci.*, 20(11), 2747(2019), DOI(<https://doi.org/10.3390/ijms20112747>)
2. D. Kharaghani, Preparation and in-vitro assessment of hierarchical organized antibacterial breath mask based on polyacrylonitrile/silver (PAN/AgNPs) nanofiber, *Nanomaterials*, 8(7), 461(2018), DOI(<https://doi.org/10.3390/nano8070461>)
3. S. Kamalesh, P. Tan, J. Wang, T. Lee, E. Kang, C. Wang, Biocompatibility of electroactive polymers in tissues, *J. Biomed. Mater. Res. An Off. J. Soc. Biomater. Japanese Soc. Biomater. Aust. Soc. Biomater. Korean Soc. Biomater.*, 52(3), 467–478(2000), DOI([https://doi.org/10.1002/1097-4636\(20001205\)52:3%3C467::AID-JBM4%3E3.0.CO;2-6](https://doi.org/10.1002/1097-4636(20001205)52:3%3C467::AID-JBM4%3E3.0.CO;2-6))
4. P. Boomi, H. G. Prabu, J. Mathiyarasu, Synthesis, characterization and antibacterial activity of polyaniline/Pt–Pd nanocomposite, *Eur. J. Med. Chem.*, 72, 18–25(2014), DOI(<https://doi.org/10.1016/j.ejmech.2013.09.049>)
5. S. Liu, Antibacterial activity of graphite, graphite oxide, graphene oxide, and reduced graphene oxide: membrane and oxidative stress, *ACS Nano*, 5(9), 6971–6980(2011), DOI([10.1021/nn202451x](https://doi.org/10.1021/nn202451x))
6. K. A. Whitehead, Antimicrobial activity of graphene oxide-metal hybrids, *Int. Biodeterior. Biodegradation*, 123, 182–190(2017), DOI(<https://doi.org/10.1016/j.ibiod.2017.06.020>)
7. B. Cao, S. Cao, P. Dong, J. Gao, J. Wang, High antibacterial activity of ultrafine TiO₂/graphene sheets nanocomposites under visible light irradiation, *Mater. Lett.*, 93, 349–352, (2013), DOI(<https://doi.org/10.1016/j.matlet.2012.11.136>)
8. O. Akhavan, E. Ghaderi, K. Rahimi, Adverse effects of graphene incorporated in TiO₂ photocatalyst on minuscule animals under solar light irradiation, *J. Mater. Chem.*, 22(43), 23260–23266(2012), DOI(<https://doi.org/10.1039/C2JM35228A>)
9. T. Kavitha, A. I. Gopalan, K. P. Lee, S. Y. Park, Glucose sensing, photocatalytic and antibacterial properties of graphene–ZnO nanoparticle hybrids, *Carbon N. Y.*,



- 50(8),2994–3000(2012),DOI(<https://doi.org/10.1016/j.carbon.2012.02.082>)
10. H. R. Pant, A green and facile one-pot synthesis of Ag–ZnO/RGO nanocomposite with effective photocatalytic activity for removal of organic pollutants, *Ceram. Int.*, 39(5), 5083–5091(2013),DOI(<https://doi.org/10.1016/j.ceramint.2012.12.003>)
11. M. Roberson, V. Rangari, S. Jeelani, T. Samuel, C. Yates, Synthesis and characterization silver, zinc oxide and hybrid silver/zinc oxide nanoparticles for antimicrobial applications, *Nano Life*, 4(1),1440003(2014), DOI(<https://doi.org/10.1142/S1793984414400030>)
12. R. M. Mohsen, S. M. M. Morsi, M. M. Selim, A. M. Ghoneim, H. M. El-Sherif, Electrical, thermal, morphological, and antibacterial studies of synthesized polyaniline/zinc oxide nanocomposites, *Polym. Bull.*, 76, 1–21(2019), DOI(<https://doi.org/10.1007/s00289-018-2348-4>)
13. M. Tariq, Green synthesis of ZnO@ GO nanocomposite and its' efficient antibacterial activity, *Photodiagnosis Photodyn. Ther.*, 35, 102471(2021), DOI(<https://doi.org/10.1016/j.pdpdt.2021.102471>)
14. L. Zhong, K. Yun, Graphene oxide-modified ZnO particles: synthesis, characterization, and antibacterial properties, *Int. J. Nanomedicine*, 10(sup1), 79–92(2015), DOI(<https://doi.org/10.2147/IJN.S88319>)
15. A. N. Abd, A. H. Al-Agha, M. A. Alheety, Addition of some primary and secondary amines to graphene oxide, and studying their effect on increasing its electrical properties, *Baghdad Sci. J.*, 13(1), (2016), DOI(<http://dx.doi.org/10.21123/bsj.2016.13.1.0097>)
16. A. H. Al-Agha, I. A. Latif, The Study of Functionalization Effect (poly aniline (PAni) and thiocarbohydrazide (TCH)) on Electrical Properties of Graphene Oxide Nanoparticles, *Diyala J. Pure Sci.*, 12(3-part 1), (2016)
17. O. G. Hammoodi, E. T. B. Al-Tikrity, K. H. Hassan, Synthesis and Characterization of Cobalt Ferrite/Graphene for The Removal of Sulfur from Kerosene by Oxidative Desulfurization, *Diyala J. Pure Sci.*, 15(3), (2019)
18. O. G. Hammoodi, E. T. B. Al-Tikrity, K. H. Hassan, Sulfur Removal from Iraqi



- Kerosene by Oxidative Desulfurization Using Cobalt Molybdate-Graphene Composite, World, 8(1), 92–99(2019)
19. A. H. Majeed, E. T. B. Al-Tikrity, D. H. Hussain, Dielectric properties of synthesized ternary hybrid nanocomposite embedded in poly (vinyl alcohol) matrix films, Polym. Polym. Compos., 29(7), 1089–1100(2021), DOI(<https://doi.org/10.1177/0967391120951406>)
20. A. A. Khalil, A. F. Shaaban, M. M. Azab, A. A. Mahmoud, A. M. Metwally, Synthesis, characterization and morphology of polyanthranilic acid micro- and nanostructures, J. Polym. Res., 20, 1–10(2013), DOI(<https://doi.org/10.1007/s10965-013-0142-4>)
21. N. F. Alheety, Antiproliferative and antimicrobial studies of novel organic-inorganic nanohybrids of ethyl 2-((5-methoxy-1H-benzo [d] imidazol-2-yl) thio) acetate (EMBIA) with TiO₂ and ZnO, J. Mol. Struct., 1274, 134489(2023), DOI(<https://doi.org/10.1016/j.molstruc.2022.134489>)
22. A. H. Majeed, D. H. Hussain, E. T. B. Al-Tikrity, M. A. Alheety, Poly (o-Phenylenediamine-GO-TiO₂) nanocomposite: modulation, characterization and thermodynamic calculations on its H₂ storage capacity, Chem. Data Collect., 28, 100450(2020), DOI(<https://doi.org/10.1016/j.cdc.2020.100450>)
23. G. Nagaraju, S. A. Prashanth, M. Shastri, K. V Yathish, C. Anupama, D. Rangappa, Electrochemical heavy metal detection, photocatalytic, photoluminescence, biodiesel production and antibacterial activities of Ag–ZnO nanomaterial, Mater. Res. Bull., 94, 54–63 (2017), DOI(<https://doi.org/10.1016/j.materresbull.2017.05.043>)
24. Q. T. Ain, S. H. Haq, A. Alshammari, M. A. Al-Mutlaq, M. N. Anjum, The systemic effect of PEG-nGO-induced oxidative stress in vivo in a rodent model, Beilstein J. Nanotechnol., 10(1), 0901–911(2019), DOI(<https://doi.org/10.3762/bjnano.10.91>)
25. M. A. Alheety, A. H. Majeed, A. H. Ali, L. A. Mohammed, A. Destagul, P. K. Singh, Synthesis and characterization of eggshell membrane polymer-TiO₂ nanocomposite for newly synthesized ionic liquid release, J. Iran. Chem. Soc., 1–11(2022), DOI(<https://doi.org/10.1007/s13738-022-02584-x>)



26. P. Jayakrishnan, M. T. Ramesan, Synthesis, structural, magnetoelectric and thermal properties of poly (anthranilic acid)/magnetite nanocomposites, *Polym. Bull.*, 74, 3179–3198(2017), DOI(<https://doi.org/10.1007/s00289-016-1883-0>)
27. L. A. Adnan, N. F. Alheety, A. H. Majeed, M. A. Alheety, H. Akbaş, Novel organic-inorganic nanohybrids (MnO₂ and Ag nanoparticles functionalized 5-methoxy-2-mercaptobenzimidazole): One step synthesis and characterization, *Mater. Today Proc.*, 42, 2700–2705(2021), DOI(<https://doi.org/10.1016/j.matpr.2020.12.707>)
28. K. Ogura, H. Shiigi, M. Nakayama, A. Ogawa, Thermal properties of poly (anthranilic acid)(PANA) and humidity-sensitive composites derived from heat-treated PANA and poly (vinyl alcohol), *J. Polym. Sci. Part A Polym. Chem.*, 37(23), 4458–4465(1999), DOI([https://doi.org/10.1002/\(SICI\)1099-0518\(19991201\)37:23%3C4458::AID-POLA23%3E3.0.CO;2-R](https://doi.org/10.1002/(SICI)1099-0518(19991201)37:23%3C4458::AID-POLA23%3E3.0.CO;2-R))